Investigation of the shape of the dots in laser irradiated crystal and PMMA using optical coherence tomography

Sohee Park, Youngseop Kim, and Yongjin Shin*

Department of Physics, Chosun University, Gwangju, 501-759, South Korea

1. Introduction

Laser engraving is the process of producing the fine grooves on the substrate to form the characters or objects. The desired characters/objects are realized by the shallow and continuous grooves. These grooves result from the evaporation of the substrate surface where laser is irradiated.[1] Laser Engraving is free of the surface residues and does not require post process polishing. Also, the 2- or 3-dimentional manipulation with laser engraving is relatively easy and it allows the high quality engraving without affecting the surface. The application of laser engraving on 2D or 3D image formation inside the crystal has been pursued recently.[2] However, due to the crystal' s low tolerance against the shock, high density and cost it is desirable to develop alternative material for the substrate.[3,4] Such an alternative is PMMA(polymethyl methacryslate). PMMA has comparable refractive index (1.495), which is the key parameter for the optimal laser engraving.

The purpose of this study is to investigate the optimal engraving conditions using PMMA. The dot engravings on two material were analyzed using the optical microscopy (OM) and optical coherence tomography (OCT) images. We used Q-switched 2nd harmonic Nd:YAG laser (wavelength = 532nm) for the engraving. The pulse energy and frequency of the laser are 26.9mJ and 50~60Hz, respectively. 6×3mm 2D image was engraved 1 mm inside the sample by irradiating the laser at 100~150 μm spatial resolution. The analysis of the dot image on the sample

was performed every 10 μm axially using OCT[5,6] and the surface images were analyzed with the OM (x 140).

2. Procedure and sample preparation

Laser 3D Engraving System (ELS-02; Proscan Co., Lagerlechfeld, Germany) controls Q-switched Nd:YAG laser and Windows™-based software Sculptor in real time to engrave the 2D or 3D images in the transparent optical glass, crystal, or polymer. This system transfers 2D or 3D images from the software (3-D Studio Max, Auto-Cad, Adobe Photoshop, or Corel Photo-Paint) to the transparent optical glass, crystal, and polymer. Laser 3D Engraving System (ELS-02) operates at 220V, 50-60Hz, and 16A.

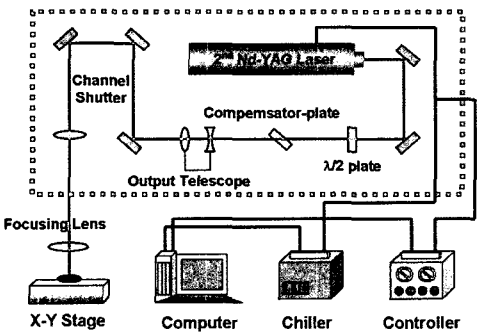

Fig. 1 Schematic of laser 3D engraving system.

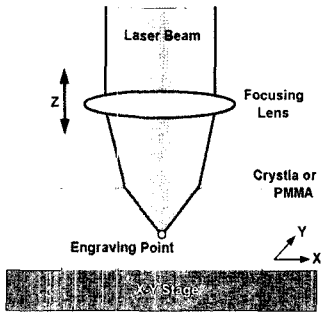

Fig. 2 Diagram of laser engraving inside object.

The high light transmission of the sample crystal results in high degree of the transparency even at large thickness. Since the glass with a higher refractive index possesses the larger reflectivity and brilliancy, we used the crystal with oxidized lead for its high refractive index. The sample PMMA is strong, light, and transparent. Also, its durability and surface hardness are superior to other alternative material for the engraving. The physical properties of crystal and PMMA are listed in Table 1.

3. Experimental

We used *Corel Photo-paint* and *Adobe Photoshop* programs for 2D image rendering.

Table 1 Physical properties of Crystal and PMMA

Classification	Crystal	PMMA
Refractive Index	1.519	1.495
Absorption coefficient (%)	0.3	0.3
Photo-transmittance (%)	< 92	92
Tensile Strength (kg/cm^2)	1,000	720
Modulus of elasticity (kg/cm^2)	about 1/3 of steel	32,000
Specific Gravity	1.19	1.18

The same six images from the 1-Bit black and white bitmap file (6mm×3mm) were irradiated pixel by pixel onto the crystal and PMMA. The laser irradiation was adjusted depending on the refractive index of respective samples. The distance between the pixels were fixed at 100 μm and the laser irradiation was performed using the biconvex focusing lens (f = 43 mm).

After laser irradiation, samples were imaged using OCT. A schematic of the OCT system is shown in Figure 3. A low coherent light source was coupled into the 2×2 fiber coupler and split into two paths. One beam was directed toward the disk and the other to a reference mirror. The light source has an output power of 10 mW at a central wavelength of 1310 nm with a bandwidth of 70 nm. A visible (633 nm) aiming beam was used to find and locate the exact imaging position on the disk. In the reference arm, a rapid-scanning optical delay line was used that employs a grating to control the phase and group delays separately so that no phase modulation is generated when the group delay was scanned.[5,6] The phase modulation was generated through an electro-optic phase modulator that produces a carrier frequency. The axial line-scanning rate was 400 Hz, and the modulation frequency of the phase modulator was 500 kHz. Reflected beams from the two arms of the interferometer were recombined in the fiber coupler and detected on a photodetector. The detected optical interference fringe intensity signals were band-pass filtered at the carrier frequency. Resultant signals were then digitized with an analog-digital converter and transferred to a computer where the structural image was generated. The lateral and axial resolutions of the reconstructed image were both 10 μm.

4. Results and discussion

In figures 4 and 5, the dot engravings in crystal and PMMA were imaged using the optical microscopy (x 140) to observe the variation in image formation as a function of the laser power. With crystal, the size of the dots and the distance between dots were consistent.

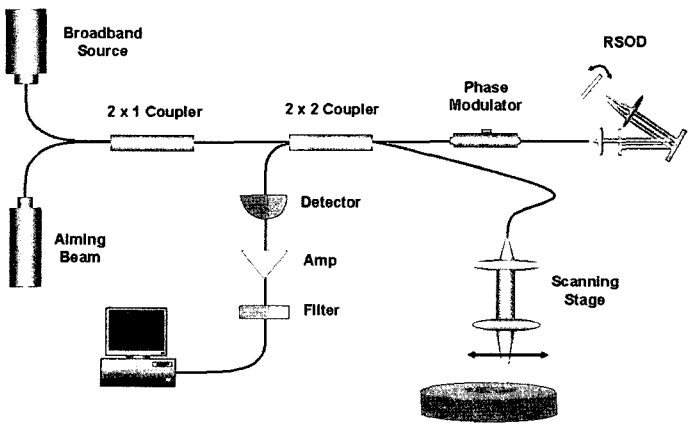

Fig. 3 Schematic of OCT imaging system: RSOD, rapid-scanning optical delay.

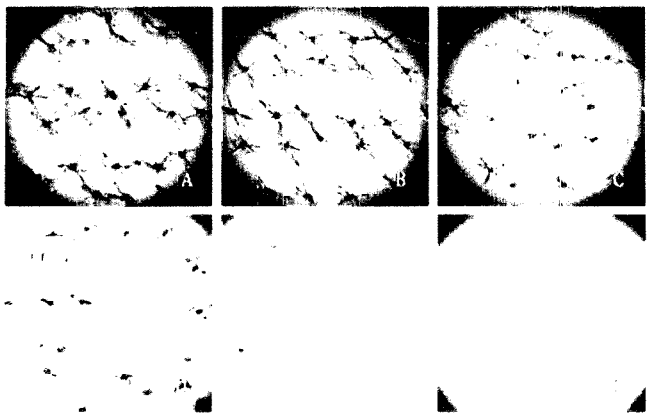

Fig. 4 Changes in crystal as a function of laser power (LC; Lamp Current %), OM images : (A) LC=90% (18~20mJ) (B) 80% (17~18mJ) (C) 70% (15~16mJ) (D) 60% (13~14mJ) (E) 50% (12~13mJ) (F) 40% (10~12mJ).

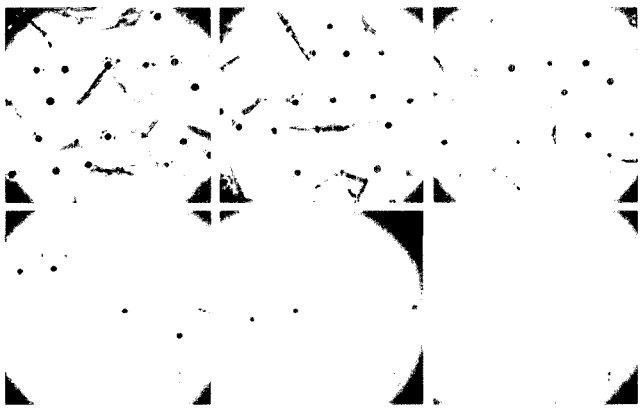

Fig. 5 Changes in PMMA as a function of laser power (LC; Lamp Current %), OM images : (A) LC=90% (18~20mJ) (B) 80% (17~18mJ) (C) 70% (15~16mJ) (D) 60% (13~14mJ) (E) 50% (12~13mJ) (F) 40% (10~12mJ).

However, the laser irradiation created sizeable cracks around the dots. Also, the size of the dots diminished fast with the lower laser output power. On the contrary, with PMMA, not only the size and the distance between dots were consistent, but the shape of the dots was nearly circular. When compared to the images with crystal, the laser irradiation created less cracks around the dots and produced the smaller but clear dot engraving even with low laser power. The characteristic and shape of the dots differ with crystal and PMMA laser irradiations. This result shown that Nd: YAG laser irradiation leads to better thermal expansion effect in PMMA while better crack damage effect during the interaction in crystal. Because of the crystal has the higher modulus of elasticity and tensile strength than PMMA.

The OCT system scans and produce the subsurface images of the samples (1

mm from the surface) with the high spatial resolution of 1~15 μm. Considering the physical properties of crystal and PMMA, the repeated OCT scans were performed every 10 μm and the dot engraving inside the samples were imaged to show the changes due to the variation in laser power. The respective OCT images from crystal and PMMA are compared in figures 6 and 7. OCT images showed that the slice of crystal has higher distribution of cracks than that of PMMA. The lower laser power created the ghost images rather than clear dot engraving. The OCT images of PMMA show otherwise.

Figure 8 shows the photograph of 3D laser engraving image inside crystal and PMMA. The comparably clear images can be produced with PMMA with simple manipulation of production parameters, which includes the use of longer wavelength (1064 nm), reduction of laser power and other adjustments with the software.

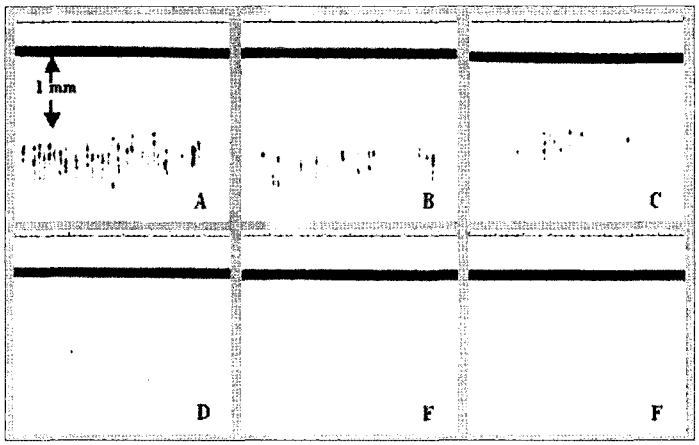

Fig. 6 Changes in crystal as a function of laser power (LC; Lamp Current %), Images were acquired using OCT: (A) LC=90% (18~20mJ) (B) 80% (17~18mJ) (C) 70% (15~16mJ) (D) 60% (13~14mJ) (E) 50% (12~13mJ) (F) 40% (10~12mJ).

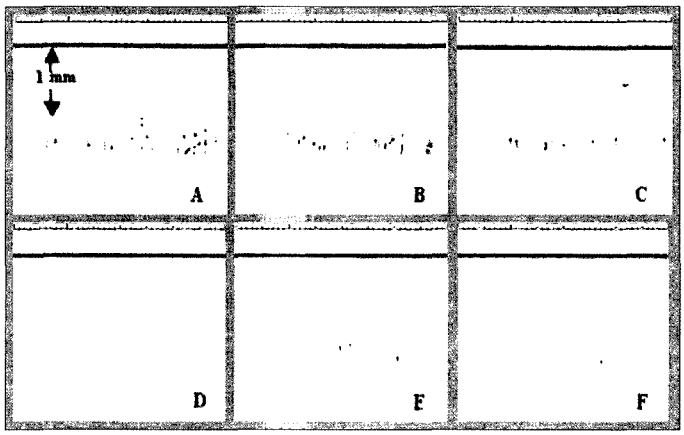

Fig. 7 Changes in PMMA as a function of laser power (LC; Lamp Current %), Images were acquired using OCT: (A) LC=90% (18~20mJ) (B) 80% (17~18mJ) (C) 70% (15~16mJ) (D) 60% (13~14mJ) (E) 50% (12~13mJ) (F) 40% (10~12mJ).

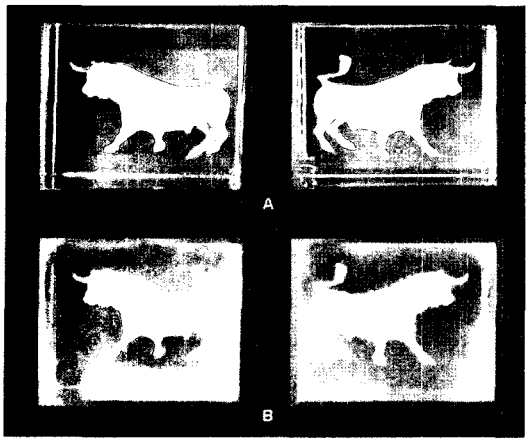

Fig. 8 Photograph of 3D laser engraving image inside (A) crystal and (B) PMMA.

5. Conclusions

The laser engravings were performed 1 mm inside crystal and PMMA sample. The output power of the laser was varied from LC=40% (10~12mJ) to LC= 90% (18~20mJ). The resulting dot engravings were imaged using OM (x 140) and OCT for the comparisons. We chose OCT as the imaging modality because it provides the high resolution (1~15 μm) axial tomographic view.

The analysis using OM and OCT images shows that PMMA is less prone to the crack formation around the dot engraving as in crystal. The low laser output power did not affect the image formation inside PMMA as much as inside crystal. PMMA was also free of the ghost images which prevented the clear image formation inside crystal.

We conclude that PMMA can be used as an alternative to crystal for the laser engraving. The comparably clear images can be produced with PMMA with simple manipulation of production parameters, which includes the use of 1064 nm wavelength, reduction of laser power and other adjustments with the software. We believe PMMA has great commercial potential as well.

References

1. W. L. Smith, "Laser-Induced Breakdown in Optical Materials," *Opt. Eng.*, **17**, p. 489, 1978.
2. Y. Kwata, H. Ueki, Y. Hashimoto, and S. Kawato, "Three-dimensional optical memory with a photorefrective crystal" *Applied Optics*, **34**, pp. 4105-4110, 1995.
3. R. M. O'Connell, T. F. Deaton, and T. T. Saito, "Single-and multiple-shot laser-damage properties of commercial grade PMMA." *Applied Optices*, **23**, pp. 682-688, 1984.
4. Y. Z.Li and Y. T. Chou, "Controlled generation of internal cracks in polymethyl methacrylate," *Materials Science and Engineering*, **A194**, pp. 113-119, 1994.
5. G. J. Tearney, B. E. Bouma, and F. G. Fujimoto, "High-speed phase- and group-delay scanning with a grating-based phase control delay line," *Opt. Lett.*, **22**, pp. 1811-1813, 1997.
6. A. M. Rollins, M. D. Kulkarnis, S. Yazdanfar, R. Ung-arunyawee, and J. A. Izatt, "In vivo video rate optical coherence tomography," *Opt. Express.*, **3**, pp. 219-229, 1998.